P−C Bond Activation and Phenyl Group Transfer in the Reaction of $Co_4(CO)_9$(mesitylene) with 2,3-Bis(diphenylphosphino)maleic Anhydride (bma). X-ray Diffraction Structures and Redox Properties of $Co_3(CO)_7[\mu_2\text{-}\eta^2,\eta^1\text{-}P(Ph)C{=}C(PPh_2)C(O)OC(O)]$ and $Co_3(CO)_6(PPh_3)[\mu_2\text{-}\eta^2,\eta^1\text{-}P(Ph)C{=}C(PPh_2)C(O)OC(O)]$

Chun-Gu Xia

Lanzhou Institute of Chemical Physics, Academia Sinica, Lanzhou 730000, PRC

Kaiyuan Yang, Simon G. Bott,* and Michael G. Richmond*

Center for Organometallic Research and Education, Department of Chemistry, University of North Texas, Denton, Texas 76230

Received May 23, 1996[⊗]

The reaction of the tetracobalt cluster $Co_4(CO)_9$(mesitylene) (**1**) with the diphosphine ligand 2,3-bis(diphenylphosphino)maleic anhydride (bma) affords the recently characterized dinuclear compounds $Co_2(CO)_2(bma)_2$ (**2**) and $Co_2(CO)_2(bma)[\mu\text{-}C{=}C(PPh_2)C(O)OC(O)](\mu_2\text{-}PPh_2)$ (**3**), in addition to the two new tricobalt clusters $Co_3(CO)_7[\mu_2\text{-}\eta^2,\eta^1\text{-}P(Ph)C{=}C(PPh_2)C(O)OC(O)]$ (**4**) and $Co_3(CO)_6(PPh_3)[\mu_2\text{-}\eta^2,\eta^1\text{-}P(Ph)C{=}C(PPh_2)C(O)OC(O)]$ (**5**) in low yields. The PPh_3-substituted cluster **5** has also been isolated, albeit in irreproduceably low yields, when $Co_2(CO)_8$ was employed as the organometallic starting material. Clusters **4** and **5** have been isolated by preparative chromatography and characterized in solution (IR and ^{31}P NMR). Evidence for bma ligand activation by P−Ph bond cleavage and the transfer of the phenyl group to a transient μ_2-PPh_2 center to form the PPh_3 ligand in **5** are confirmed by X-ray diffraction analysis. The redox behavior of **4** and **5** has been explored in CH_2Cl_2, and these data are discussed relative to the results obtained from extended Hückel molecular orbital calculations. Electrochemical and molecular orbital comparisons between cluster **4** and the related carbene-bridged cluster $Co_3(CO)_6[\mu_2\text{-}\eta^2,\eta^1\text{-}C(Ph)C{=}C(PPh_2)C(O)OC(O)](\mu_2\text{-}PPh_2)$ (**6**) are presented.

Introduction

The activation of phosphine ligands by polynuclear cluster compounds has been extensively explored over the last several years, with special interest aimed at gaining a greater understanding of the selectivity exhibited by such systems in the cleavage of the groups attached to the phosphine ligand.[1] In the case of the cluster-coordinated H_2PR and HPR_2 ligands, the predominant activation pathway involves P−H bond cleavage, while the coordination of trialkyl(or aryl)phosphines typically leads to P−C bond activation.[1] Studies dealing with cluster activation of mixed phosphines having the form $PR_{3-n}R'_n$ (where $R \neq R'$; $n = 1, 2$) reveal that the ease of P−C bond cleavage is dependent on the hybridization of the attached carbon atom, decreasing in the order P−C(sp) > P−C(sp^2) > P−C(sp^3).[2] An interesting situation arises when the ancillary phosphine ligand contains two or three different groups, all of which have the same hybridization. Here it is not immediately clear whether any group selectivity exists in the P−C bond cleavage reaction, especially in the case of the redox-active ligands bma and 4,5-bis(diphenylphosphino)-4-cyclopentene-1,3-dione (bpcd), which we have employed in our studies dealing with the preparation of new cluster/ligand redox systems. These two diphosphines can undergo P−C bond activation at either the phenyl group (P−Ph) or the five-membered anhydride or dione ring (P-ring).[3] Unfortunately, data relating to the kinetics and thermodynamics are not known for the oxidative addition of the P−C bond at either mono- or polynuclear metal centers. These data are valuable, as they would enable researchers, in theory, to better predict the course of metal-induced ligand degradation reactions involving phosphine ligands.

Our interest in the area of phosphine ligand activation derives from the unexpected reaction between the tricobalt clusters $RCCo_3(CO)_9$ (where R = Ph, ferrocenyl) and the redox-active ligand bma.[4,5] The substitution of

[⊗] Abstract published in *Advance ACS Abstracts,* September 15, 1996.

(1) (a) Lavigne, G. In *The Chemistry of Metal Cluster Complexes*; Shriver, D. F., Kaesz, H. D., Adams, R. D., Eds.; VCH Publishers: New York, 1990; Chapter 5. (b) Garrou, P. E. *Chem. Rev.* **1985**, *85*, 171.

(2) Carty, A. J. *Pure Appl. Chem.* **1982**, *54*, 113.

(3) For examples of electronic effects in P−C bond scission reactions, see: (a) Dubois, R. A.; Garrou, P. E. *Organometallics* **1986**, *5*, 466. (b) Abatjoglou, A. G.; Bryant, D. R. *Organometallics* **1984**, *3*, 932.

(4) Yang, K.; Smith, J. M.; Bott, S. G.; Richmond, M. G. *Organometallics* **1993**, *12*, 4779.

S0276-7333(96)00401-3 CCC: $12.00

two CO groups by the diphosphine ligand affords the intermediate cluster $RCCo_3(CO)_7(bma)$, which upon thermolysis or near-UV irradiation experiences an activation of the P−C(maleic anhydride) bond, coupled with reductive C−C bond formation between the capping-benzylidyne ligand and the transient Co−C(maleic anhydride) moiety, to give cluster $Co_3(CO)_6[\mu_2\text{-}\eta^2,\eta^1\text{-}C(R)C{=}C(PPh_2)C(O)OC(O)](\mu_2\text{-}PPh_2)$ (**6**). Equation 1

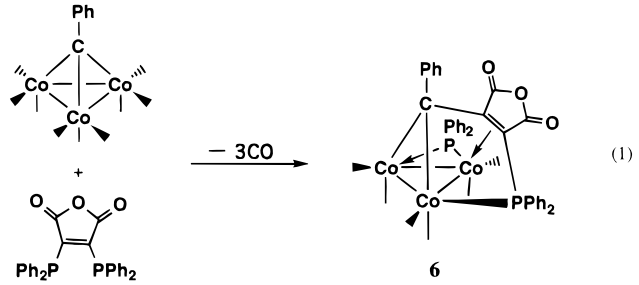

(1)

6

shows the net reaction between the phenyl-capped nonacarbonyl cluster and bma. While the clusters $RCCo_3(CO)_9$ (where R = H, Me) readily react with added bma to give the product of simple substitution, $RCCo_3(CO)_7(bma)$, continued heating leads to extensive decomposition and no sign of the corresponding phosphido-bridged cluster (*vide supra*).[6]

We have begun to examine the reactivity of both bma and bpcd with other polynuclear systems in order to more fully understand the scope of the redox chemistry and bond-breaking processes exhibited by these two particular ligands upon cluster coordination.[7] One logical avenue for the extension of our tricobalt work involves the replacement of the capping-benzylidyne ligand, making use of the isolobal analogy,[8] and examination of the resulting chemistry as a function of the incorporated isolobal fragment. Accordingly, we have explored the reaction between the tetracobalt cluster $Co_4(CO)_9$(mesitylene) and bma and have found that the introduction of the Co(mesitylene) fragment in place of the carbyne moiety RC leads to very different ligand activation chemistry. The observation of $Co_4(CO)_9$(mesitylene) fragmentation and phenyl-group transfer from the bma ligand illustrates the gross differences that exist between the tri- and tetrametal tetrahedrane clusters. Herein we report our data on the reactivity of $Co_4(CO)_9$(mesitylene) with bma, along with the characterization of the isolable products $Co_2(CO)_2(bma)_2$ (**2**) and $Co_2(CO)_2(bma)[\mu\text{-}C{=}C(PPh_2)C(O)OC(O)](\mu_2\text{-}PPh_2)$ (**3**), $Co_3(CO)_7[\mu_2\text{-}\eta^2,\eta^1\text{-}P(Ph)C{=}C(PPh_2)C(O)OC(O)]$ (**4**), and $Co_3(CO)_6(PPh_3)[\mu_2\text{-}\eta^2,\eta^1\text{-}P(Ph)C{=}C(PPh_2)C(O)OC(O)]$ (**5**). The former two dinuclear compounds have recently been obtained from the reaction of the diyne compound $[Co_2(CO)_6]_2(PhC_4Ph)$ with added bma.[9] The new clusters $Co_3(CO)_7[\mu_2\text{-}\eta^2,\eta^1\text{-}P(Ph)C{=}C(PPh_2)C(O)OC(O)]$ (**4**) and $Co_3(CO)_6(PPh_3)[\mu_2\text{-}\eta^2,\eta^1\text{-}P(Ph)C{=}C(PPh_2)C(O)OC(O)]$ (**5**) (where the descriptors μ_2, η^2, and η^1 refer to the bridging phosphido, maleic anhydride, and phosphine groups, respectively, associated with the maleic anhydride ring) have been fully characterized in solution and by X-ray diffraction analysis. The effect of the coordinated maleic anhydride ring on the redox properties of clusters **4** and **5** has been assessed by cyclic voltammetric methods, and the data are compared to the molecular orbital information obtained from extended Hückel calculations.

Scheme 1

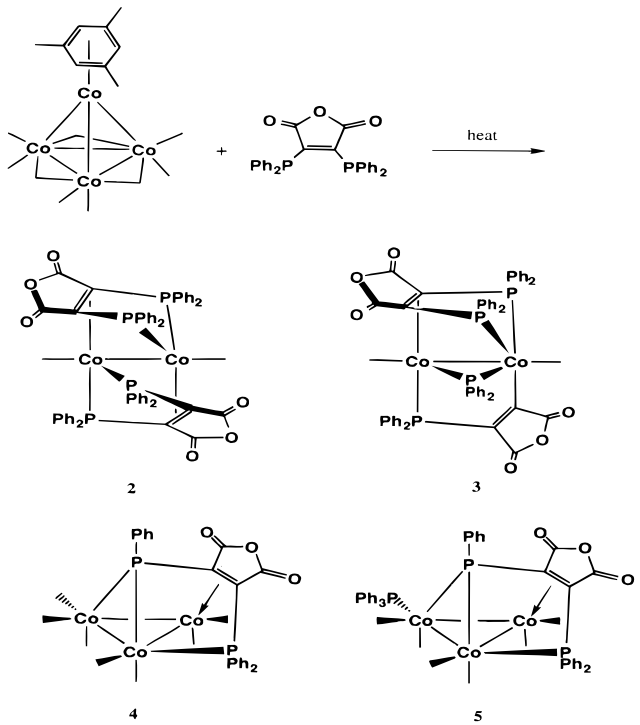

Results and Discussion

I. Synthesis and X-ray Diffraction Structures for $Co_3(CO)_7[\mu_2\text{-}\eta^2,\eta^1\text{-}P(Ph)C{=}C(PPh_2)C(O)OC(O)]$ (4) and $Co_3(CO)_6(PPh_3)[\mu_2\text{-}\eta^2,\eta^1\text{-}P(Ph)C{=}C(PPh_2)C(O)OC(O)]$ (5).

Thermolysis of the cluster $Co_4(CO)_9$(mesitylene) with the diphosphine ligand bma at 75 °C in toluene overnight leads to four observable products by TLC analysis, along with the presence of a small amount of unreacted **1** and a large amount of decomposition. Attempts to achieve ligand substitution under milder reaction conditions using the oxidative-decarbonylation reagent Me_3NO were not successful. The thermolysis products were isolated by column chromatography over silica gel. Two of the four products were determined to be the dinuclear compounds $Co_2(CO)_2(bma)_2$ (**2**) and $Co_2(CO)_2(bma)[\mu\text{-}C{=}C(PPh_2)C(O)OC(O)](\mu_2\text{-}PPh_2)$ (**3**), whose identities have been unequivocally established by us.[9] The two, new remaining products proved be the trinuclear clusters **4** and **5**, as depicted in Scheme 1.

The IR spectrum of cluster **4** exhibits terminal carbonyl bands at 2078 (s), 2038 (vs), 2017 (m, sh), and

(5) Shen, H.; Bott, S. G.; Richmond, M. G. *Inorg. Chim. Acta*, in press.

(6) Unpublished results.

(7) (a) Xia, C.-G.; Bott, S. G.; Richmond, M. G. *Inorg. Chim. Acta* **1995**, *230*, 45. (b) Shen, H.; Williams, T. J.; Bott, S. G.; Richmond, M. G. *J. Organomet. Chem.* **1995**, *505*, 1.

(8) (a) Hoffmann, R. *Angew. Chem., Int. Ed. Engl.* **1982**, *21*, 711. (b) Stone, F. G. A. *Angew. Chem., Int. Ed. Engl.* **1984**, *23*, 89.

(9) Yang, K.; Martin, J. A.; Bott, S. G.; Richmond, M. G. *Organometallics* **1996**, *15*, 2227.

Table 1. X-ray Crystallographic Data and Processing Parameters for $Co_3(CO)_7[\mu_2\text{-}\eta^2,\eta^1\text{-}P(Ph)C{=}C(PPh_2)C(O)OC(O)]$ (4) and $Co_3(CO)_6(PPh_3)[\mu_2\text{-}\eta^2,\eta^1\text{-}P(Ph)C{=}C(PPh_2)C(O)OC(O)]$ (5)

	4	5
space group	$P2_1/n$, monoclinic	$P2_1/n$, monoclinic
a, Å	10.4877(8)	15.0487(8)
b, Å	17.0865(9)	15.771(1)
c, Å	17.224(1)	18.026(1)
β, deg	105.394(6)	92.853(6)
V, Å^3	2975.8(4)	4272.9(5)
mol formula	$C_{29}H_{15}Co_3O_{10}P_2$	$C_{46}H_{30}Co_3O_9P_3$
fw	762.18	996.47
formula units per cell (Z)	4	4
ρ, g·cm^{-3}	1.701	1.549
abs coeff (μ), cm^{-1}	18.11	13.14
λ(Mo Kα), Å	0.710 73	0.710 73
collcn range, deg	$2.0 \le 2\theta \le 44.0$	$2.0 \le 2\theta \le 44.0$
max scan time, s	120	120
scan speed range, deg·min^{-1}	0.67−8.0	0.67−8.0
tot. no. of data collcd	4026	5691
no. of indep data, $I > 3\sigma(I)$	2229	2327
R	0.0417	0.0488
R_w	0.0442	0.0539
GOF	0.72	0.63
weights	$[0.04F^2 + (\sigma(F)^2]^{-1}$	$[0.04F^2 + (\sigma(F)^2]^{-1}$

1957 (w) cm^{-1}, along with two ν(CO) bands for the anhydride moiety appearing at 1812 (w) and 1749 (m) cm^{-1},[10] while the ^{31}P NMR spectrum consists of two resonances at δ 170.0 and 23.4, assignable to the μ_2-phosphido and the PPh_2(maleic anhydride) moieties, respectively. Cluster **5**, with its added electron density due to the PPh_3 ligand, shows the expected shift to lower energy of all the carbonyl stretching bands relative to cluster **4**. In **5** the terminal Co−CO bands are found at 2052 (vs), 2022 (vs), 2003 (m), and 1991 (m) cm^{-1}, and the anhydride ν(CO) bands are observed at 1801 (w) and 1741 (m) cm^{-1}. The three ^{31}P resonances recorded for **5** at δ 157.7, 54.1, and 26.3 are assigned to the bridging μ_2-phosphido, PPh_3, and PPh_2(maleic anhydride) groups, respectively. Treatment of **4** with added PPh_3 at 40 °C in toluene provided high yields of **5**, suggesting that the introduction of PPh_3 into **5** most likely derives from a liberated PPh_3 ligand that subsequently attacks **4**. It should be noted that in this case no evidence was observed for the existence of other regioisomers in this control substitution reaction.

We have also found that bma reacts with $Co_2(CO)_8$ to give cluster **5** in low yield as the sole isolable product. We have confirmed by IR spectroscopy that the first intermediate is that of $Co(CO)_3$(bma),[11] which is fairly temperature sensitive and decomposes over the course of the reaction. The extensive decomposition and irreproduceability associated with this reaction makes a detailed study problematic, and further mechanistic studies were not pursued.

(10) Dolphin, D.; Wick, A. *Tabulation of Spectral Data*; Wiley-Interscience: New York, 1977.

(11) (a) Fenske, D. *Chem. Ber.* **1979**, *112*, 363. (b) Mao, F.; Tyler, D. R.; Keszler, D. *J. Am. Chem. Soc.* **1989**, *111*, 130. (c) Mao, F.; Tyler, D. R.; Bruce, M. R.; Bruce, A. E.; Rieger, A. L.; Rieger, P. H. *J. Am. Chem. Soc.* **1992**, *114*, 6418. (d) Tyler, D. R. *Acc. Chem. Res.* **1991**, *24*, 325.

Table 2. Selected Bond Distances (Å) and Angles (deg) in $Co_3(CO)_7[\mu_2\text{-}\eta^2,\eta^1\text{-}P(Ph)C{=}C(PPh_2)C(O)OC(O)]$ (4) and $Co_3(CO)_6(PPh_3)[\mu_2\text{-}\eta^2,\eta^1\text{-}P(Ph)C{=}C(PPh_2)C(O)OC(O)]$ (5)[a]

$Co_3(CO)_7[\mu_2\text{-}\eta^2,\eta^1\text{-}P(Ph)C{=}C(PPh_2)C(O)OC(O)]$ (**4**)

Bond Distances

Co(1)−Co(2)	2.558(2)	Co(1)−Co(3)	2.595(2)
Co(2)−Co(3)	2.581(1)	Co(1)−P(1)	2.215(2)
Co(1)−P(2)	2.150(3)	Co(1)−C(1)	1.776(9)
Co(1)−C(2)	1.799(9)	Co(2)−C(3)	1.787(9)
Co(2)−C(4)	1.798(9)	Co(2)−C(11)	2.044(7)
Co(2)−C(15)	2.048(8)	Co(3)−P(2)	2.139(2)
Co(3)−C(5)	1.78(1)	Co(3)−C(6)	1.79(1)
Co(3)−C(7)	1.797(9)	P(1)−C(11)	1.804(9)
P(2)−C(15)	1.784(8)	O(1)−C(1)	1.13(1)
O(2)−C(2)	1.13(1)	O(3)−C(3)	1.14(1)
O(4)−C(4)	1.13(1)	O(5)−C(5)	1.15(1)
O(6)−C(6)	1.12(1)	O(7)−C(7)	1.12(1)
O(12)−C(12)	1.18(1)	O(13)−C(12)	1.41(1)
O(13)−C(14)	1.40(1)	O(14)−C(14)	1.18(1)
C(11)−C(12)	1.47(1)	C(11)−C(15)	1.43(1)
C(14)−C(15)	1.47(1)		

Bond Angles

Co(2)−Co(1)−Co(3)	60.11(4)	Co(1)−Co(2)−Co(3)	60.65(4)
Co(1)−Co(3)−Co(2)	59.24(4)	P(1)−Co(1)−P(2)	91.99(9)
C(11)−Co(2)−C(15)	40.8(3)	Co(1)−P(2)−Co(3)	74.44(8)
Co(1)−P(2)−C(211)	127.1(3)	Co(3)−P(2)−C(211)	127.9(3)
Co(1)−C(1)−O(1)	177.2(9)	Co(1)−C(2)−O(2)	177.0(9)
Co(2)−C(3)−O(3)	177.4(8)	Co(2)−C(4)−O(4)	178.8(8)
Co(3)−C(5)−O(5)	178.2(8)	Co(3)−C(6)−O(6)	178.6(8)
Co(3)−C(7)−O(7)	178.2(8)		

$Co_3(CO)_6(PPh_3)[\mu_2\text{-}\eta^2,\eta^1\text{-}P(Ph)C{=}C(PPh_2)C(O)OC(O)]$ (**5**)

Bond Distances

Co(1)−Co(2)	2.613(2)	Co(1)−Co(3)	2.518(2)
Co(2)−Co(3)	2.615(2)	Co(1)−P(1)	2.194(4)
Co(1)−P(2)	2.189(3)	Co(1)−C(1)	1.79(1)
Co(1)−C(2)	1.77(1)	Co(2)−C(3)	1.82(1)
Co(2)−C(4)	1.76(1)	Co(2)−C(11)	2.04(1)
Co(2)−C(15)	2.06(1)	Co(3)−P(2)	2.163(3)
Co(3)−P(3)	2.190(4)	Co(3)−C(5)	1.72(1)
Co(3)−C(6)	1.74(1)	P(1)−C(11)	1.81(1)
P(2)−C(15)	1.77(1)	O(1)−C(1)	1.15(2)
O(2)−C(2)	1.13(2)	O(3)−C(3)	1.13(1)
O(4)−C(4)	1.16(2)	O(5)−C(5)	1.19(2)
O(6)−C(6)	1.15(2)	O(12)−C(12)	1.19(2)
O(13)−C(12)	1.39(1)	O913)−C(14)	1.38(1)
O(14)−C(14)	1.19(1)	C(11)−C(12)	1.47(2)
C(11)−C(15)	1.42(2)	C(14)−C(15)	1.51(1)

Bond Angles

Co(2)−Co(1)−Co(3)	61.27(6)	Co(1)−Co(2)−Co(3)	57.58(6)
Co(1)−Co(3)−Co(2)	61.15(6)	P(1)−Co(1)−P(2)	92.2(1)
C(11)−Co(2)−C(15)	40.6(4)	Co(1)−Co(3)−P(2)	55.1(1)
Co(1)−Co(3)−P(3)	155.3(1)	Co(2)−Co(3)−P(3)	131.2(1)
Co(1)−P(2)−Co(3)	70.7(1)	Co(1)−P(2)−C(211)	123.0(4)
Co(3)−P(2)−C(211)	133.4(4)	Co(1)−C(1)−O(1)	179(1)
Co(1)−C(2)−O(2)	178(1)	Co(2)−C(3)−O(3)	176(1)
Co(2)−C(4)−O(4)	177(1)	Co(3)−C(5)−O(5)	167(1)
Co(3)−C(6)−O(6)	176(1)		

[a] Numbers in parentheses are estimated standard deviations in the least significant digits.

The molecular structures of **4** and **5** were established by X-ray crystallography. Both clusters exist as discrete molecules in their unit cells with no unusually short inter- or intramolecular contacts. Table 1 shows the pertinent X-ray data collection and processing parameters, and Table 2 shows selected bond distances and angles for **4** and **5**. The ORTEP diagrams for these clusters are displayed in Figure 1.

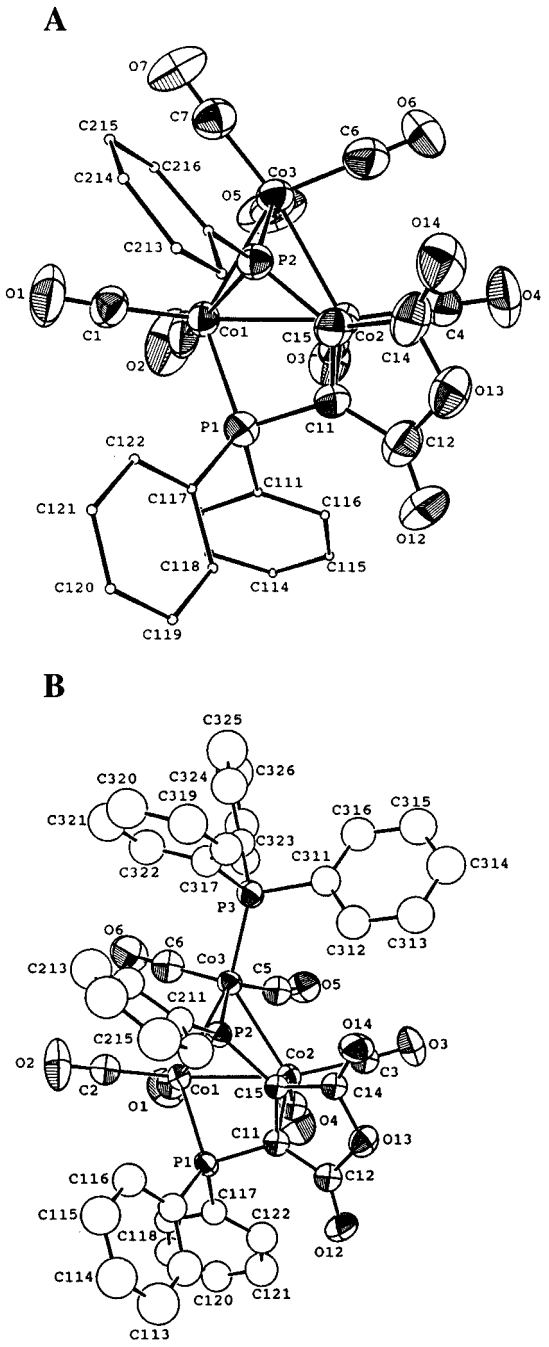

Figure 1. ORTEP diagrams for the non-hydrogen atoms of (a) $Co_3(CO)_7[\mu_2\text{-}\eta^2,\eta^1\text{-}P(Ph)C{=}C(PPh_2)C(O)OC(O)]$ (**4**) and (b) $Co_3(CO)_6(PPh_3)[\mu_2\text{-}\eta^2,\eta^1\text{-}P(Ph)C{=}C(PPh_2)C(O)OC(O)]$ (**5**), showing the thermal ellipsoids at the 50% probability level.

Both **4** and **5** are similar in structure to the recently characterized cluster $Co_3(CO)_6[\mu_2\text{-}\eta^2,\eta^1\text{-}C(Ph)C{=}C(PPh_2)C(O)OC(O)](\mu_2\text{-}PPh_2)$ (**6**),[4] and as such, only the prominent features will be discussed. Each of these new clusters contains a planar, triangular array of cobalt atoms that exhibits a mean Co−Co bond length of 2.578(2) and 2.582(2) Å, respectively, for **4** and **5**, which is in good agreement with other related Co_3 clusters of this genre,[13] in addition to possessing a seven-electron $\mu_2\text{-}\eta^2,\eta^1$-phenylphosphido(diphenylphosphino)maleic anhydride ligand, whose bond angles and distances are unexceptional with respect to other such cluster compounds reported by us.[12,14] The demonstration of a PPh_3 group in **5** clearly supports the fact that a bma ligand has undergone a P−Ph bond activation process. The origin of the PPh_3 ligand may reasonably be viewed as arising from such an oxidatively activated phenyl group that has been transferred to a transient μ_2-PPh_2 moiety at some point during the reaction. The exact timing concerning the introduction of the PPh_3 ligand in **5** cannot be ascertained at this point; however, we favor attack on cluster **4** by a liberated PPh_3 ligand during the thermolysis reaction (*vide supra*). The PPh_3 group adopts an equatorial site in **5**, as supported by a P(2)−Co(3)−P(3) bond angle of 106.9(1)°.

Scheme 2

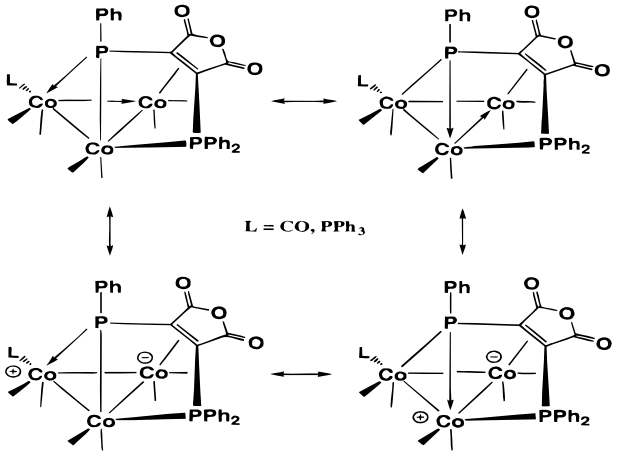

Scheme 2 shows several of the more important resonance structures that adequately describe the bonding in clusters **4** and **5**. Both zwitterionic and donor−acceptor Co−Co bonds are required if these clusters are to be viewed by using a conventional electron-counting formalism. Alternatively, both clusters may also be considered within the context of a delocalized bonding model by utilizing polyhedral skeletal electron pair (PSEP) theory.[15] Here each cluster is best viewed as a four-vertex *arachno* cluster, containing seven skeletal electron pairs (SEP). The adopted polyhedral shape in **4** and **5** is easily traced back to the corresponding six-vertex *closo* octahedral cluster that has had two adjoining vertices removed, as shown in eq 2.

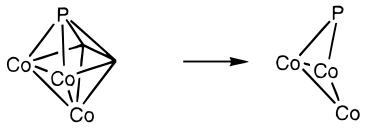

(2)

II. Cyclic Voltammetry Data. All reported cyclic voltammetric data were collected at a platinum electrode at room temperature and a scan rate of 0.1 V s^{-1} in CH_2Cl_2 containing 0.2 M tetra-*n*-butylammonium perchlorate (TBAP) as the supporting electrolyte. Table

(12) Yang, K.; Bott, S. G.; Richmond, M. G. *Organometallics* **1994**, *13*, 3767.

(13) (a) Watson, W. H.; Nagl, A.; Hwang, S.; Richmond, M. G. *J. Organomet. Chem.* **1993**, *445*, 163. (b) Yang, K.; Bott, S. G.; Richmond, M. G. *J. Organomet. Chem.* **1993**, *454*, 273.

(14) Yang, K.; Bott, S. G.; Richmond, M. G. *Organometallics* **1995**, *14*, 919, 2718.

(15) (a) Mingos, D. M. P.; May, A. S. In *The Chemistry of Metal Cluster Complexes*; Shriver, D. F., Kaesz, H. D., Adams, R. D., Eds.; VCH Publishers: New York, 1990; Chapter 2. (b) Mingos, D. M. P.; Wales, D. J. *Introduction to Cluster Chemistry*; Prentice Hall: Englewood Cliffs, NJ, 1990.

Table 3. Cyclic Voltammetry Data for Compounds 4−6[a]

	redox couple[b]										
		0/1−					1−/2−				
compd	E_{p^a}	E_{p^c}	E_{p^a}	I_{p^a}/I_{p^c}	ΔE_p	$E_{1/2}$	E_{p^c}	E_{p^a}	I_{p^a}/I_{p^c}	ΔE_p	$E_{1/2}$
4	1.15	−0.63	−0.55	1.0	0.08	−0.59	−1.31	−0.90		0.40	
5	0.83	−0.90	−0.82	1.0	0.08	−0.87	−1.63	−1.29		0.34	
6	0.83	−0.55	−0.46	1.0	0.09	−0.51	−1.17	−1.01	1.0	0.16	−1.09

[a] In ca. 10^{-3} M CH_2Cl_2 solutions containing 0.2 M TBAP at room temperature and a scan rate of 0.1 V s^{-1}. Potentials are in volts relative a silver-wire quasi-reference electrode, calibrated against Cp_2Fe. [b] E_{p^a} and E_{p^c} refer to the anodic and cathodic peak potentials of the CV waves. The half-wave potential $E_{1/2}$, which represents the chemically reversible redox couple, is defined as $(E_{p^a} + E_{p^c})/2$. [c] CVs remained irreversible under all conditions examined.

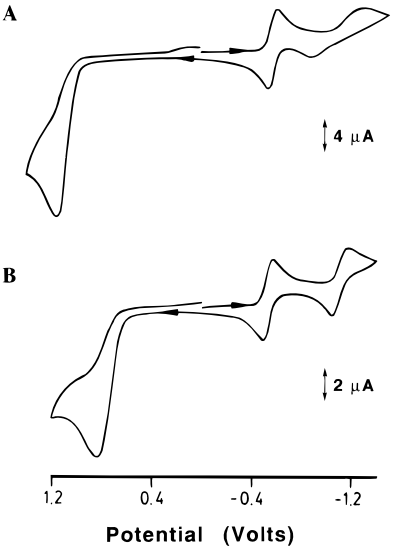

Figure 2. Cathodic scan cyclic voltammograms of (a) $Co_3(CO)_7[\mu_2\text{-}\eta^2,\eta^1\text{-}P(Ph)C{=}C(PPh_2)C(O)OC(O)]$ (**4**) and (b) $Co_3(CO)_6[\mu_2\text{-}\eta^2,\eta^1\text{-}C(Ph)C{=}C(PPh_2)C(O)OC(O)](\mu_2\text{-}PPh_2)$ (**6**) (ca. 10^{-3} M) at 298 K in CH_2Cl_2 containing 0.2 M TBAP at 0.1 V s^{-1}.

3 summarizes the electrochemical data for **4**−**6**, and Figure 2 shows the cyclic voltammograms (CV) of **4** and **6**.

Removal of an electron from the HOMO of **4** leads to an irreversible oxidation wave displaying an E_{p^a} value of 1.15 V. Increasing the scan rates up to of 5 V s^{-1} and lowering the temperature to −40 °C did not lead to any noticeable return redox couple (E_{p^c}), and further redox examination of the oxidation was abandoned. The two reduction waves observed may be assigned to the 0/1− and 1−/2− redox couples. The diffusion-controlled and reversible nature of the 0/1− redox couple, which exhibits an $E_{1/2} = -0.59$ V, has been confirmed by standard electrochemical methods,[16] and the electron stoichiometry has been verified by calibration of the peak current against a known amount of added ferrocene using Walden's rule.[17] The peak-to-peak separation of 400 mV and the diminished current ratio ($I_{p^a}/I_{p^c} < 1$) associated with the second reduction in **4** signals the intervention of a structural rearrangement or a slow electron transfer (i.e., k_{het} low), of which we favor the former possibility (*vide infra*).[18] The overall uptake of two electrons in related tetrahedrane clusters has been shown to occur at the occupation of antibonding metal framework orbitals, followed by cluster fragmentation.[19]

The redox behavior of the PPh_3-substituted derivative **5** mirrors that of **4**. The replacement of a CO group by the better donor ligand PPh_3 leads to a ca. 0.25 V shift to more negative potential of the three redox responses in **5** relative to **4**.[20] All of the redox assignments previously discussed for cluster **4** may be extended to **5** given the close structural relationship between these two clusters.

In comparison to clusters **4** and **5** that contain a bridging phosphido(maleic anhydride) ligand, the benzylidene(maleic anhydride)-substituted cluster **6** exhibits very similar electrochemical properties, showing an irreversible oxidation wave at $E_{p^a} = 0.83$ and the two reduction couples (0/1− and 1−/2−).[21,22] There is, however, one pronounced difference that involves the 1−/2− redox couple, which is seen (Table 3 and Figure 2) to be reversible in the case of **6**. We believe that the greater stability of $\mathbf{6}^{2-}$ relative to the dianions of **4** and **5** has its origin in the nature of the amount of overlap between the π^* orbital of the maleic anhydride moiety and the tricobalt frame, as discussed more fully in the following section.

III. Extended Hückel Calculations. The composition of the HOMO and LUMO levels in clusters **4** and **6** was probed by carrying out extended Hückel molecular orbital calculations on the model compounds $Co_3(CO)_7[\mu_2\text{-}\eta^2,\eta^1\text{-}P(H)C{=}C(PH_2)C(O)OC(O)]$ and $Co_3(CO)_6[\mu_2\text{-}\eta^2,\eta^1\text{-}C(H)C{=}C(PH_2)C(O)OC(O)](\mu_2\text{-}PH_2)$. Figure 3

(16) The usual criteria for determining diffusion control (current function plots) and redox-couple reversibility (ΔE_p and current ratios) have been applied. See: (a) Rieger, P. H. *Electrochemistry*; Chapman & Hall: New York, 1994. (b) Adams, R. N. *Electrochemistry at Solid Electrodes*; Marcel Dekker: New York, 1969.

(17) Bard, A. J.; Faulkner, L. R. *Electrochemical Methods*; Wiley: New York, 1980.

(18) A reviewer has proposed that the anodic couple at −1.31 V corresponds to the oxidation of a product arising from the decomposition of the dianion. While this is a possibility, steady-state CVs show no evidence for any new cathodic wave(s) (E_{p^c}) associated with the suggested decomposition product(s). Moreover, if the decomposition of the dianion was the predominant pathway, one would not expect to see the current ratio of near unity that we find with the first reduction step (Figure 2a).

(19) (a) Matheson, T. W.; Peake, B. M.; Robinson, B. H.; Simpson, J.; Watson, D. J. *J. Chem. Soc., Chem. Commun.* **1973**, 894. (b) Peake, B. M.; Robinson, B. H.; Simpson, J.; Watson, D. J. *Inorg. Chem.* **1977**, *16*, 405. (c) Bond, A. M.; Peake, B. M.; Robinson, B. H.; Simpson, J.; Watson, D. J. *Inorg. Chem.* **1977**, *16*, 410. (d) Beurich, H.; Madach, T.; Richter, F.; Vahrenkamp, H. *Angew. Chem.* **1979**, *91*, 751. (e) Lindsay, P. N.; Peake, B. M.; Robinson, B. H.; Simpson, J.; Honrath, U.; Vahrenkamp, H.; Bond, A. M. *Organometallics* **1984**, *3*, 413.

(20) (a) Yang, K.; Bott, S. G.; Richmond, M. G. *Organometallics* **1994**, *13*, 3788. (b) Richmond, M. G.; Kochi, J. K. *Inorg. Chem.* **1986**, *25*, 656.

(21) A more detailed electrochemical examination of **6** was conducted due to the higher yield associated with the synthesis of **6**. Rotating disk electrode (RDE) voltammetry has confirmed the electron stoichiometry of the two reduction waves in **6** (plot of $\log[(I_d - I)/I]$ vs E (V)) and has yielded a value of 6.29×10^{-6} cm^2 s^{-1} for the diffusion coefficient (D_o) (plot of i vs $v^{1/2}$), which is characteristic of this genre of cluster (see refs 13b and 22).

(22) Downard, A. J.; Robinson, B. H.; Simpson, J. *Organometallics* **1986**, *5*, 1140.

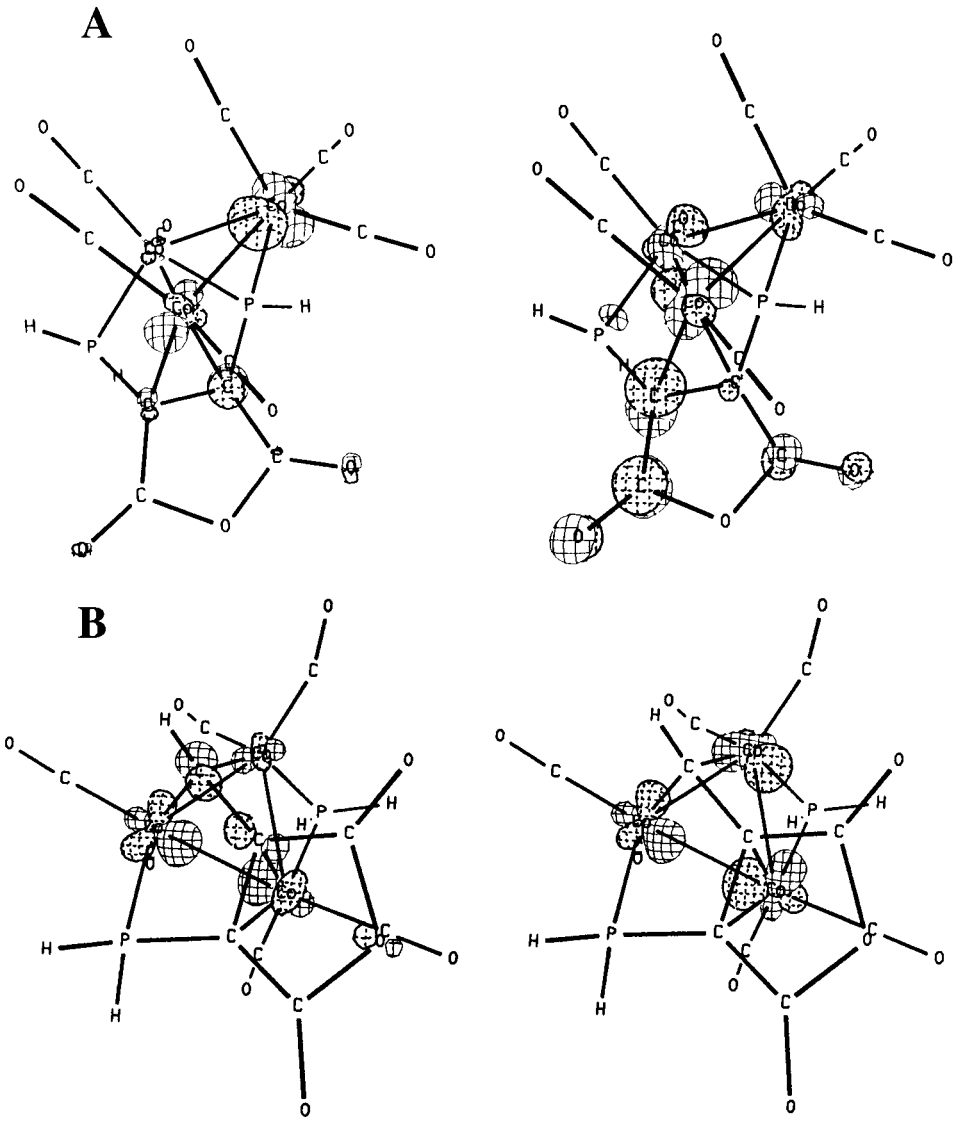

Figure 3. CACAO drawings of the HOMO (left) and the LUMO (right) for (a) $Co_3(CO)_7[\mu_2\text{-}\eta^2,\eta^1\text{-}P(H)\overline{C{=}C(PH_2)C(O)OC(O)}]$ and (b) $Co_3(CO)_6[\mu_2\text{-}\eta^2,\eta^1\text{-}C(H)\overline{C{=}C(PH_2)C(O)OC(O)}](\mu_2\text{-}PH_2)$.

shows the three-dimensional CACAO drawings of the orbitals of interest.[23]

The HOMO of $Co_3(CO)_7[\mu_2\text{-}\eta^2,\eta^1\text{-}P(H)\overline{C{=}C(PH_2)C(O)OC(O)}]$ occurs at −11.62 eV and reveals a major antibonding interaction between two of the cobalt centers (52%), along with minor interactions involving the CO groups (17%) and the C=C π bond of the maleic anhydride moiety (8%). This particular π bond experiences a net bonding interaction with the cobalt center. The LUMO is found at −10.53 eV and consists of nearly equal contributions from the maleic anhydride group (30%) and the tricobalt frame (35%). The σ-antibonding interaction that exists between the three cobalt atoms is analogous to the a_2 LUMO found by Schilling and Hoffmann in their study of M_3L_9(ligand) clusters.[24] The nodal pattern of the maleic anhydride moiety is similar to that of ψ_4 in other six-π-electron compounds,[25] except for the reduced π contribution at one of the ring carbon atoms, which serves to intensify the antibonding interaction between the carbon and cobalt centers.

The methylidene-ligated cluster $Co_3(CO)_6[\mu_2\text{-}\eta^2,\eta^1\text{-}C(H)\overline{C{=}C(PH_2)C(O)OC(O)}](\mu_2\text{-}PH_2)$ reveals a HOMO at −11.87 eV that is composed of Co−Co interactions (51%) that are overall σ bonding in nature. The apparent σ bond formed between the methylidene and maleic anhydride carbons (5%) clearly overlaps with the Co_3 frame in an antibonding manner. The a_2 LUMO found in $Co_3(CO)_6[\mu_2\text{-}\eta^2,\eta^1\text{-}C(H)\overline{C{=}C(PH_2)C(O)OC(O)}](\mu_2\text{-}PH_2)$ displays an energy of −10.57 eV and is identical in all respects to the LUMO found by us in $Co_3(CO)_4(PMe_3)_2[\mu_2\text{-}\eta^2,\eta^1\text{-}C(H)\overline{C{=}C(PH_2)C(O)OC(O)}](\mu_2\text{-}PH_2)$[14] and $Co_3(CO)_6[\mu_2\text{-}\eta^2,\eta^1\text{-}C(\text{ferrocenyl})\overline{C{=}C(PH_2)C(O)OC(O)}](\mu_2\text{-}PH_2)$.[5] The contribution of the three cobalt atoms amounts to 60%. With the exception of the contribution of the maleic anhydride π^* system to $Co_3(CO)_7[\mu_2\text{-}\eta^2,\eta^1\text{-}P(H)\overline{C{=}C(PH_2)C(O)OC(O)}]$, the LUMOs of both model cluster compounds examined here are identical.[26]

(23) Mealli, C.; Proserpio, D. M. *J. Chem. Educ.* **1990**, *67*, 399.
(24) Schilling, B. E. R.; Hoffmann, R. *J. Am. Chem. Soc.* **1979**, *101*, 3456.
(25) Albright, T. A.; Burdett, J. K.; Whangbo, M. H. *Orbital Interactions in Chemistry*; Wiley: New York, 1985.

We believe that the MO calculations provide a rationale for the apparent stability difference between $\mathbf{6}^{2-}$ and $\mathbf{4}^{2-}$. Given the unfavorable maleic anhydride π^*-Co interaction present in the LUMO of **4**, a scheme involving the dissociation of the C=C bond of maleic anhydride ring from the cluster would not be unreasonable and could serve as a starting locus for the irreversible CV wave that accompanies the second reduction step. Equation 3 shows this particular dissociation

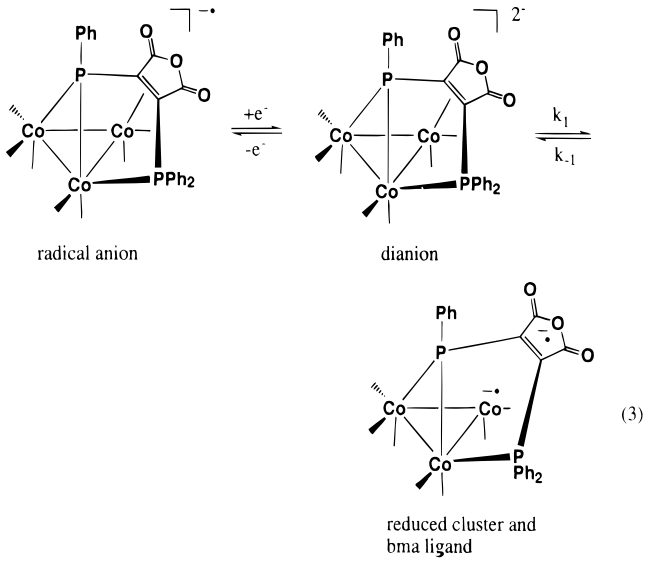

(3)

scenario. In the EC reaction depicted in eq 3 it is assumed that the dissociative release of the maleic anhydride C=C bond from the cluster frame is rapid after the second reduction step. Since the three cobalt centers and the bma residue possess superior electron reservoir properties, a possible driving force that may be at work here is the greater delocalization of the odd-electron density over two spatially separated redox centers. The tethering of such a "coordinatively flexible" cluster/ligand system may actually afford novel redox-active systems that are stable under a wider variety of conditions. This premise continues to be explored in our laboratories. We note that this proposed mode of cluster flexibility would not be available to $Co_3(CO)_6[\mu_2\text{-}\eta^2,\eta^1\text{-}C(H)\overline{C{=}C(PH_2)C(O)OC(O)}](\mu_2\text{-}PH_2)$ due to the absence of this particular maleic anhydride π^*-Co_3 interaction in the LUMO.

Conclusions

Through our characterization of clusters **4** and **5** we have shown that the bma ligand undergoes both P−C(maleic anhydride) and P−C(phenyl) bond cleavages, and in the case of the latter process, the cobalt-bound phenyl group is ultimately transferred to μ_2-PPh_2 moiety at some point during the reaction to give the PPh_3 ligand found in cluster **5**. The redox behavior of **4** and **5** was explored by cyclic voltammetry and the concept of a "coordinatively flexible" maleic anhydride moiety that can provide additional assistance in the stabilization of reduced clusters presented.

Experimental Section

General Procedures. $Co_4(CO)_9$(mesitylene) was synthesized according to the published procedure,[27] using $Co_2(CO)_8$ that was purchased from Strem Chemical Co. The bma ligand used was prepared from 2,3-dichloromaleic anhydride and $PPh_2(SiMe_3)$, using the procedure of Tyler.[28] The solvents toluene and pentane were distilled from Na/benzophenone, while CH_2Cl_2 was distilled from P_2O_5. Standard Schlenk techniques were employed in the handling and storage of all solvents.[29] The TBAP (*caution:* strong oxidant!) used in the CV studies was obtained from Johnson Matthey Electronics and recrystallized from ethyl acetate/petroleum ether, after which it was dried under vacuum for 2 days. All quoted microanalyses were performed by Atlantic Microlab, Inc., Norcross, GA.

Infrared spectra were recorded on a Nicolet 20SXB FT-IR spectrometer in sealed 0.1 mm NaCl cells. The ^{13}C and ^{31}P NMR spectra were recorded on a Varian 300-VXR spectrometer at 75 and 121 MHz, respectively. The ^{31}P NMR data were referenced to external H_3PO_4 (85%), taken to have $\delta = 0$, with positive chemical shifts signifying resonances that are low field to the external standard.

Reaction of $Co_4(CO)_9$(mesitylene) with bma. To a Schlenk tube containing 0.50 g (0.82 mmol) of $Co_4(CO)_9$(mesitylene) and 0.84 g (1.8 mmol) of bma was added 60 mL of toluene by syringe, after which the vessel was heated overnight at 75 °C. TLC analysis of the cooled solution confirmed the presence of four products, in addition to a trace amount of $Co_4(CO)_9$(mesitylene). The toluene was removed under vacuum, and the crude reaction mixture was purified by column chromatography over silica gel. The first band of green $Co_4(CO)_9$(mesitylene) (50 mg) was eluted from the column using CH_2Cl_2/petroleum ether (2:8), followed by a second green band that corresponded to cluster **4** (60 mg), after the solvent system was changed to a 1:1 mixture of CH_2Cl_2/petroleum ether. Two additional bands were obtained by using CH_2Cl_2/petroleum ether (3:1), which were determined to be the dinuclear compound **2** (orange color; band 3; 55 mg) and cluster **5** (green color; band 4; 10 mg). The last compound isolated was **3** (45 mg), which was obtained as band five (brown color) using CH_2Cl_2 as the eluant.[30] Samples of **4** and **5** suitable for microanalysis and X-ray diffraction analysis were obtained from solutions containing CH_2Cl_2 that had been layered with pentane.

Cluster 4. IR (CH_2Cl_2): ν(CO) 2078 (s), 2038 (vs), 2017 (m, sh), 1957 (w), 1812 (w, asymm bma C=O), 1749 (m, symm bma C=O) cm^{-1}. $^{31}P\{^1H\}$ NMR (CH_2Cl_2, −90 °C): δ 170.0, 23.4. Anal. Calcd (found) for $C_{29}H_{15}Co_3O_{10}P_2 \cdot {}^1/_2CH_2Cl_2$: C, 44.00 (44.11); H, 1.99 (2.04).

Cluster 5. IR (CH_2Cl_2): ν(CO) 2052 (vs), 2022 (vs), 2003 (m), 1991 (m), 1801 (w, asymm bma C=O), 1741 (m, symm bma C=O) cm^{-1}. $^{31}P\{^1H\}$ NMR (CH_2Cl_2, −90 °C): δ 157.7, 54.1, 26.3. Anal. Calcd (found) for $C_{46}H_{30}Co_3O_9P_3$: C, 55.45 (55.17); H, 3.03 (3.06).

Synthesis of $Co_3(CO)_6(PPh_3)[\mu_2\text{-}\eta^2,\eta^1\text{-}P(Ph)\overline{C{=}C(PPh_2)C(O)OC(O)}]$ (5) from PPh_3 and $Co_3(CO)_7[\mu_2\text{-}\eta^2,\eta^1\text{-}P(Ph)\overline{C{=}C}$-

(26) (a) The LUMOs of both of the model clusters are separated by ca. 0.7 eV from the next unoccupied molecular orbital, removing any doubt as to which MO is occupied upon formation of the radical anion and dianion. Further proof concerning the occupation of Co−Co antibonding orbitals upon reduction comes the IR spectra of both $\mathbf{4}^-$ and $\mathbf{6}^-$. Here the low-frequency shift of the terminal CO groups (ca. 40−80 cm^{-1}) upon electron accession is much larger than the ca. 20−30 cm^{-1} found in the maleic anhydride ring. This indicates that the maleic ring is not the predominant site of reduction. (b) Cf.: Yang, K.; Bott, S. G.; Richmond, M. G. *Organometallics* **1995**, *14*, 2387.

(27) Kaganovich, V. S.; Rybinskaya, M. I. *J. Organomet. Chem.* **1988**, *344*, 383.

(28) Mao, F.; Philbin, C. E.; Weakley, T. J. R.; Tyler, D. R. *Organometallics* **1990**, *9*, 1510.

(29) Shriver, D. F. *The Manipulation of Air-Sensitive Compounds*; McGraw-Hill: New York, 1969.

(30) Due the problematic nature in determining the percent yield in such a cluster fragmentation reaction, we have only reported the weight amount of isolated material.

$(PPh_2)C(O)OC(O)]$ (4). To 50 mg (0.066 mmol) of $Co_3(CO)_7[\mu_2\text{-}\eta^2,\eta^1\text{-}P(Ph)C{=}C(PPh_2)C(O)OC(O)]$ in a Schlenk tube containing 24 mg (0.085 mmol) of PPh_3 was added 15 mL of toluene, after which the Schlenk tube was heated at 40 °C for 2.0 h. The completion of the reaction was ascertained by TLC analysis and IR spectroscopy. At this point the toluene was removed under vacuum and $Co_3(CO)_6(PPh_3)[\mu_2\text{-}\eta^2,\eta^1\text{-}P(Ph)C{=}C(PPh_2)C(O)OC(O)]$ was isolated by column chromatography using CH_2Cl_2 as the eluant. Yield: 58 mg (89%).

Thermolysis Reaction of $Co_2(CO)_8$ with bma. To a Schlenk tube containing 0.25 g (0.73 mmol) of $Co_2(CO)_8$ and 0.18 g (0.39 mmol) of bma was added 25 mL of toluene via cannula. The solution was next heated overnight at reflux, followed by cooling to room temperature. TLC analysis at this point revealed the presence of only a tiny amount of $Co_3(CO)_6(PPh_3)[\mu_2\text{-}\eta^2,\eta^1\text{-}P(Ph)C{=}C(PPh_2)C(O)OC(O)]$ along with a large amount of decomposition material at the origin of the TLC plate. The desired cluster was isolated as described directly above. Yield: 35 mg.

X-ray Crystallography. All X-ray data were collected on an Enraf-Nonius CAD-4 diffractometer using the $\theta/2\theta$-scan technique, Mo Kα radiation ($\lambda = 0.710\ 73$ Å), and a graphite monochromator. The procedures utilized in the data collection have been described.[31] Table 1 gives the details associated with the data collection. All data were corrected for Lorentz and polarization effects, in addition to absorption (DIFABS).[32] Both structures were solved by direct methods using SIR for **4** and SHELX-86 for **5**, and each model was refined by using full-matrix least-squares techniques. The treatment of the thermal parameters was based on the number of observed data, with anisotropic parameters incorporated for **4** (the Co, P, and all non-phenyl carbon atoms) and **5** (the Co, P, and O atoms). All hydrogen atoms were located in difference maps and were included in the final model in idealized positions ($U(H) = 1.3B_{eq}(C)$). All computations other than those specified were performed by using MoIEN,[33] with scattering factors taken from the usual source.[34]

Electrochemical Studies. The cyclic voltammograms were obtained with a PAR Model 273 potentiostat/galvanostat. All recorded CVs utilized positive feedback circuitry to compensate for *iR* drop. The airtight cyclic voltammetry cell was based on a three-electrode design, and the electrochemical experiments employed a platinum disk as the working and auxiliary electrode. The reference electrode employed in all experiments consisted of a silver-wire quasi-reference electrode, with all potential data reported relative to the formal potential of the Cp_2Fe/Cp_2Fe^+ (internally added) redox couple, taken to have $E_{1/2} = 0.307$ V.[17]

MO Calculations. The extended Hückel calculations on the model compounds $Co_3(CO)_7[\mu_2\text{-}\eta^2,\eta^1\text{-}P(H)C{=}C(PH_2)C(O)OC(O)]$ and $Co_3(CO)_6[\mu_2\text{-}\eta^2,\eta^1\text{-}C(H)C{=}C(PH_2)C(O)OC(O)](\mu_2\text{-}PH_2)$ were carried out with the original program developed by Hoffmann,[35] as modified by Mealli and Proserpio,[23] with weighted H_{ij}'s.[36] The input *Z*-matrices for $Co_3(CO)_7[\mu_2\text{-}\eta^2,\eta^1\text{-}P(H)C{=}C(PH_2)C(O)OC(O)]$ and $Co_3(CO)_6[\mu_2\text{-}\eta^2,\eta^1\text{-}C(H)C{=}C(PH_2)C(O)OC(O)](\mu_2\text{-}PH_2)$ were constructed by using the X-ray data of each cluster, followed by the replacement of all phenyl groups by hydrogen atoms using the PC modeling program MOBY. A $C(sp^2)-H$ distance of 1.07 Å was used in the calculations. All P−H bonds were set to a distance of 1.42 Å,[37] while the remaining distances and angles were taken from the X-ray data of clusters **4** and **6**.

Acknowledgment. Prof. Carlo Mealli is thanked for providing us with a copy of his CACAO drawing program, and financial support from the Robert A. Welch Foundation (Grants B-1202-SGB and B-1039-MGR) and the UNT Faculty Research Program is much appreciated.

Supporting Information Available: Textual presentations of the crystallographic experimental details, an ORTEP diagram, and listings of crystallographic data, bond distances, bond angles, and atomic positional and thermal parameters for compounds **4** and **5** (18 pages). Ordering information is given on any current masthead page.

OM960401G

(31) Mason, M. R.; Smith, J. M.; Bott, S. G.; Barron, A. R. *J. Am. Chem. Soc.* **1993**, *115*, 4971.
(32) Walker, N.; Stuart, D. *Acta Crystallogr., Sect. A* **1983**, *39*, 159.
(33) *Molen, An Interactive Structure Solution Program*; Enraf-Nonius: Delft, The Netherlands, 1990.
(34) Cromer, D. T.; Waber, J. T. *International Tables for X-ray Crystallography*; Kynoch Press: Birmingham, U.K., 1974; Vol. IV, Table 2.
(35) (a) Hoffmann, R.; Lipscomb, W. N. *J. Chem. Phys.* **1962**, *36*, 2179. (b) Hoffmann, R. *J. Chem. Phys.* **1963**, *39*, 1397.
(36) Ammeter, J. H.; Bürgi, H.-B.; Thibeault, J. C.; Hoffmann, R. *J. Am. Chem. Soc.* **1978**, *100*, 3686.
(37) Weast, R. C., Ed. *Handbook of Chemistry and Physics*, 56th ed.; CRC Press: Cleveland, OH, 1975.